*Journal of Microscopy, Vol. 229, Pt 2 2008, pp. 307–312*
*Received 28 September 2006; accepted 2 May 2007*

# Real-time monitoring of the surface relief formation on azo-polymer films upon near-field excitation

A. AMBROSIO*, A. CAMPOSEO†, P. MADDALENA*,
S. PATANÈ‡ AND M. ALLEGRINI§
*CNR-INFM CRS-COHERENTIA and Dipartimento di Scienze Fisiche, Università di Napoli 'Federico II', Via Cintia, I-80126 Napoli, Italy*
*†National Nanotechnology Laboratory CNR-INFM, Distretto tecnologico ISUFI, Via Arnesano, 73100 Lecce, Italy*
*‡Dipartimento di Fisica della Materia e Tecnologie Fisiche Avanzate, Università di Messina, Salita Sperone 31, I-98166 Messina, Italy*
*§Dipartimento di Fisica 'E. Fermi', Università di Pisa and polyLAB CNR-INFM Largo B. Pontecorvo 3, I-56127 Pisa, Italy*

**Key words.** Near-field lithography, near-field microscopy, polymer films.

## Summary

We use near-field optical microscopy to investigate the early state formation of photo-induced topographical structures on the free surface of azobenzene-containing polymers. The near-field technique is employed to monitor in real time the mass migration during the embossing of the surface of 50/50 copolymer films of polymethacrylate and polymethacrylate containing 3-methyl-4$'$-pentyloxy-azobenzene units. The dynamic of surface relief formation induced by light have been investigated as a function of the sample temperature. Furthermore, a formula derived from Navier–Stokes equations for classical laminar flow has been used to fit the mass displacement data during the embossing process. Excellent agreements between the experimental data and the fitting formula have been found for all the temperature considered.

## Introduction

In 1995 Kim *et al.* (1995a, b) first observed the change of the morphology on the surface of an epoxy-based polymer film under illumination. They were able to draw a topographical grating on the film surface by exposure to the interference pattern of two laser beams. Trenches were formed corresponding to the bright regions of the interference pattern and protrusions into the dark regions. Azo-containing polymers are known to be characterized by the formation of surface relief (SRF) upon light irradiation (Kim *et al.*, 1995). The origin of the formation of topographical features has been ascribed to the re-orientation of the azobenzene molecules and successive reorganization of the polymer chains upon light exposure. Azobenzene molecules have two possible configurations, a planar form (trans-form) and a non-planar configuration (cis-form) (Kumar & Neckers, 1998). During isomerization, azo-based molecules turn from a rod-like structure (trans form) to a bent structure (cis form). The isomerization of azobenzene molecules, both trans-cis and cis-trans, can be activated by exposure to laser light, usually in the UV/blue wavelength region. SRF is a surface effect and can be inhibited by coating the film surface with a transparent multi-layer (Viswanathan *et al.*, 1998). Topographical gratings have been realized with diffraction efficiency up to 40% (Barrett *et al.*, 1996; Jiang *et al.*, 1996), whereas topographical structures up to 1 $\mu$m thick (Kim *et al.*, 1995; Holme *et al.*, 1999) have been drawn, involving up to 50% of the film thickness (Kim *et al.*, 1995).

The drawing of topographical structures on azo-containing polymers via light exposure has been observed to largely depend on the polarization state of the writing beam as well as on the presence of an intensity gradient into the illuminating light spot (Barrett *et al.*, 1998; Bian *et al.*, 1999). In particular, if the polarization of the light is perpendicular to the direction of the intensity gradient, topographical structures cannot be grown. Topographical structures are formed when the polarization direction of the writing beam has a component along the light gradient vector. This behaviour has been attributed to polymer chain migration induced by the optical-field gradient force. Aside the polarization dependence of the process, topographical structures on azo-based polymers

Correspondence to: Antonio Ambrosio. Tel: +33 08162 6322; fax: +33 08162 6346; e-mail: tony@ne.infn.it

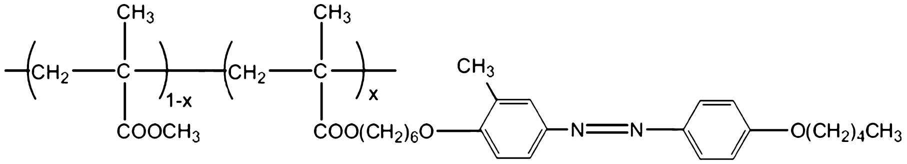

**Fig. 1.** Chemical structure of the copolymer used in this investigation, 50/50 PMA/PMA4 copolymer.

appear in regions of the sample surface where the writing laser beam exhibits an intensity gradient. This is the case of light intensity modulation of an interference pattern as well as light gradient obtained in a single focussed Gaussian beam (Bian *et al.*, 1999). A single focussed Gaussian beam has been observed to produce a hole for intensities of tens of W cm$^{-2}$ (low power regime). Nevertheless, when the power density reaches hundreds of W cm$^{-2}$ (high power regime), protrusions instead of trenches come up in the region of the brighter light (Bian *et al.*, 1999). The existence of two power regimes in SRF resulting in structures with opposite shapes is still a matter of discussion and is far from a complete solution. Several models have been proposed trying to fully explain the characteristics of the SRF formation phenomenon on azo-containing polymers. The only certain issue, up to now, is that SRF formation is activated by light and it is a consequence of the azobenzene isomerization.

Scanning near-field optical microscope (SNOM) has also been employed to draw topographical structures on the free surface of azo-based polymers with sub-wavelength resolution (Davy & Spajer, 1996; Landraud *et al.*, 2001; Hasegawa *et al.*, 2001). Those experiments have confirmed the existence of two power regimes even for near-field illumination. When the light power density is low (tens of W cm$^{-2}$), the structures locally designed by near-field illumination are trenches, and when the power density is high (hundreds of W cm$^{-2}$), the structures are protrusions. We have used SNOM to monitor, in real time, the formation of single topographical protrusions (dots) on the free surface of azobenzene-based copolymers. We worked into the high power density regime. In addition to experimental work, we found an expression based on Navier–Stokes equations for classical laminar flow that we used to describe by a best fit the experimental observations.

## Experimental procedure

We used a 50/50 copolymer of polymethacrylate, PMA, and PMA containing 3-methyl-4$'$-pentyloxy-azobenzene units connected at the 4-position of the main polymer chain via six hexamethylene spacers, PMA4, (Fig. 1). This material has already been used for near-field lithography (Patanè *et al.*, 2002; Likodimos *et al.*, 2003; Labardi *et al.* 2003). The spin-coated films are prepared from a highly concentrated solution of copolymer powder dissolved in chlorobenzene and stirred at room temperature for a few hours (Andreozzi *et al.*, 2002). Films about 200 nm thick are obtained. PMA4 shows a nematic phase below the nematic-to-isotropic temperature of $T_{NI}$ = 353 K (Andreozzi *et al.*, 2002), whereas it exhibits transition to a glassy state at the low glass transition temperature of $T_g$ = 294 K. The polymer films were excited by the 417-nm laser light from a diode laser (Nichia, Japan). This wavelength is suitable to activate trans–cis isomerization in our samples. The experimental set-up is sketched in Fig. 2 (top). The SNOM probe (commercial, by Nanonics Ltd., Israel) is an optical fibre machined and metalized at one edge to produce a conical tip ending with a sub-wavelength aperture (the nominal aperture is 50 nm, according to manufacturer-supplied information). Laser light is injected into the optical fibre and it is guided to the conical tip. Here, the light is confined towards the apical aperture by means of a metallic coating that covers the tip. Tips at the end of the fibre are usually produced by means of chemical etching or a heat and pull process, whereas the linear dimensions of the tip aperture may be obtained by monitoring the fibre throughput (the ratio between transmitted and injected light power) or producing a scanning electron microscopy micrograph of the fibre tip. The geometric characteristic of the SNOM probe leads to the loss of most of the light injected into the optical fibre owing to the absorption and reflection of the light by the metallic coating. This phenomenon leads to the heating and elongation of the probe (Ambrosio *et al.*, 2005; Gucciardi *et al.*, 2005; Latini *et al.*, 2005). The thermal behaviour of SNOM optical fibres has been carefully taken into account in the investigation reported in this paper. As sketched in Fig. 2, the SNOM optical fibre is glued on one arm of a tuning fork kept at a constant oscillation by means of a dithering piezo (not shown in figure). By monitoring the free oscillation amplitude of the tuning fork, a feedback circuit drives the piezo scanner in order to stabilize the tip-to-sample distance to a height smaller than 10 nm. Furthermore, the sample is in contact with a temperature controller that can stabilize the sample temperature in the range 15–70°C, in air conditions.

On the free surface of our samples, we draw single relief (dots) under near-field exposure (Fig. 2, bottom). The power of the light injected into the SNOM probe is of 0.1 mW, whereas the exposure time for drawing each dot is of 20 s. In near-field lithography, the dot dimensions are believed to reflect the effective size of the aperture at the end of the SNOM probe (Likodimos *et al.*, 2003). In accordance with this thought and using an estimated throughput of about $10^{-3}$ for our SNOM fibre, the light power on the sample should be about 0.1 $\mu$W, corresponding to an intensity of 200 W cm$^{-2}$. This value of the

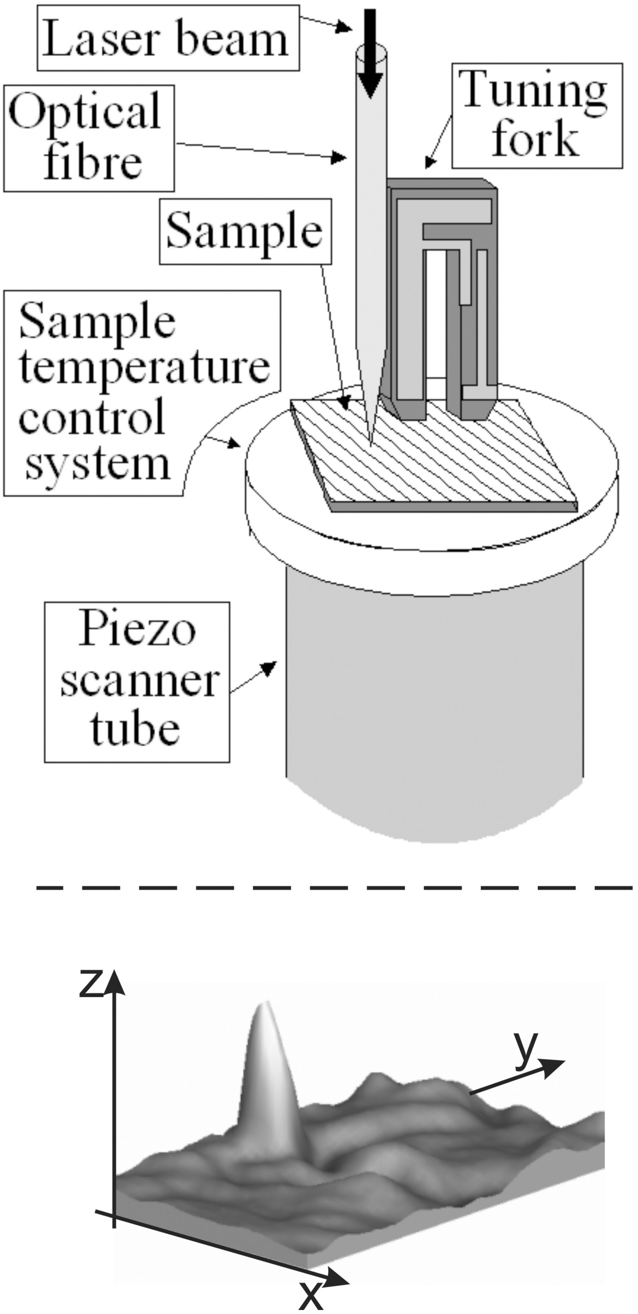

**Fig. 2.** (Top) Sketch of the SNOM set-up used for our experiment. The laser light (417 nm from a laser diode) is injected into a SNOM optical fibre machined in order to obtain a sub-wavelength aperture at the tip end. The sample is mounted on a temperature controller and it is moved by means of a piezo-scanner tube. (Bottom) 3D view of a typical dot grown on the surface of the PMA/PMA4 copolymer film. The dot height is of about 65 nm and the diameter is of about 200 nm.

intensity confirms that we worked in the high-power regime for azo-polymers. This evaluation is in accordance with the shape of the topographical structures we have drawn, that is, dots instead of holes.

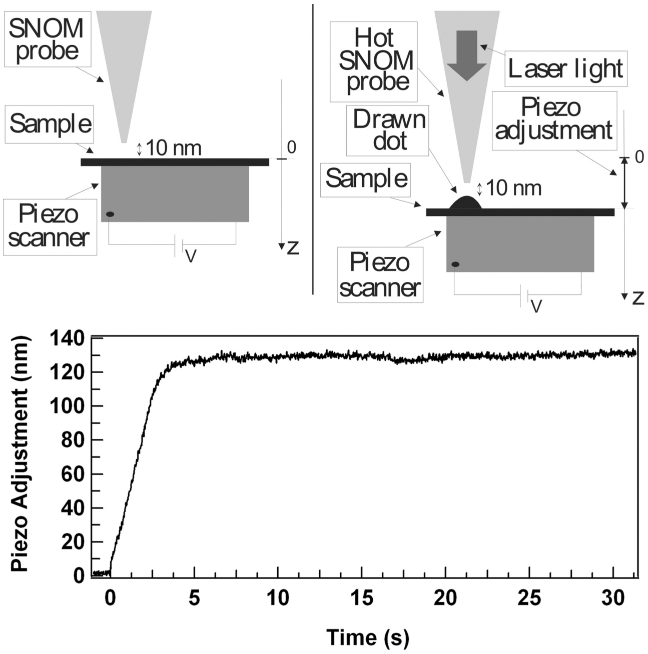

**Fig. 3.** Sketch of the experimental procedure: we first approach the tip to the sample surface (panel a). Then we inject laser light into the SNOM optical fibre (panel b) and record the feedback signal driving the piezo-scanner (trace on the bottom).

In our investigation, we have first approached the SNOM tip to the sample surface keeping the tip-to-sample distance stabilized at 10 nm by means of the feedback circuit. Then we have injected laser light into the SNOM optical fibre. After injecting laser light, the feedback circuit retracts the piezo-scanner from its original position in order to keep constant the tip-to-sample distance. In these conditions, the piezo retraction is due to the occurrence of two phenomena: (a) the elongation of the tip due to tip heating via absorption of laser light by the metal coating that covers the fibre end and (b) the growth of a dot on the sample surface under near-field illumination. We have recorded the feedback signal corresponding to the piezo retraction using a digital oscilloscope. The acquired signal thus represents a convolution of the dot growth and the tip elongation. The procedure is illustrated in Fig. 3. To neglect any effect due to the heating of the SNOM tip, we have moved the tip on the sample surface keeping the light injected into the SNOM optical fibre, that is, keeping the probe hot and elongated. Then, we have stopped the scanning, leaving a dot grown under near-field illumination. We have recorded the piezo adjustment in this condition that is now representative only of the dot formation because the tip has already elongated, as reported in Fig. 4. We have also checked that the embossing of the surface under near-field illumination is not due to heat transfer from the hot SNOM tip to the sample surface. For this check, we have injected 0.4 mW of red laser light, four times greater than the power used for 417 nm wavelength. In this

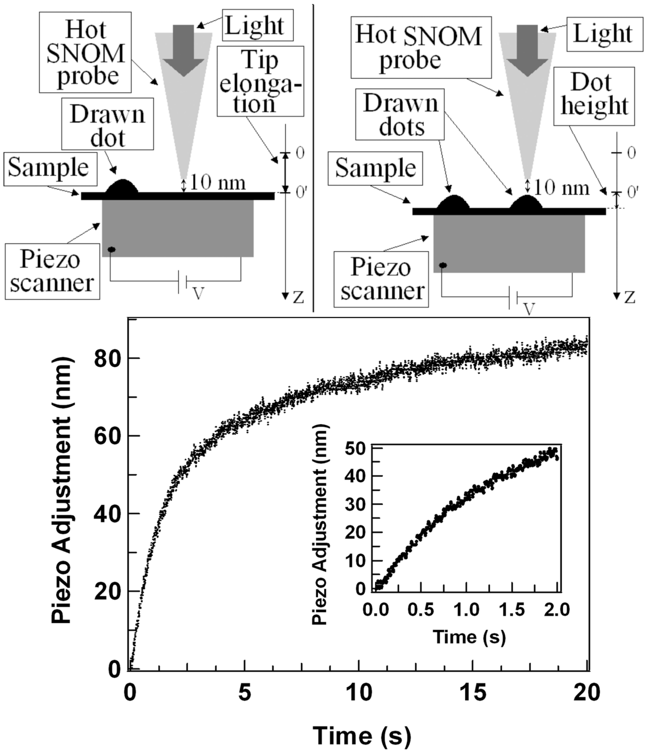

**Fig. 4.** Sketch of the data acquisition procedure: after drawing the first dot, we move the SNOM probe on the sample surface keeping the light injected into the fibre (panel a). Then we stop into a point leaving a dot growing under illumination (panel b). We record again the feedback signal corresponding to piezo-adjustment (bottom).

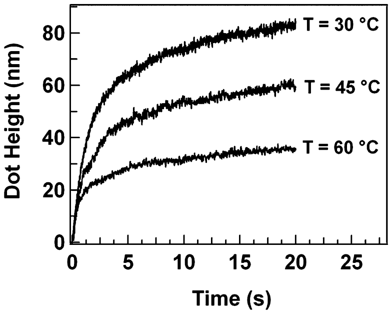

**Fig. 5.** Plots of the dot height versus the exposure time in correspondence of three different values of the sample temperature, stabilized by means of the temperature controller.

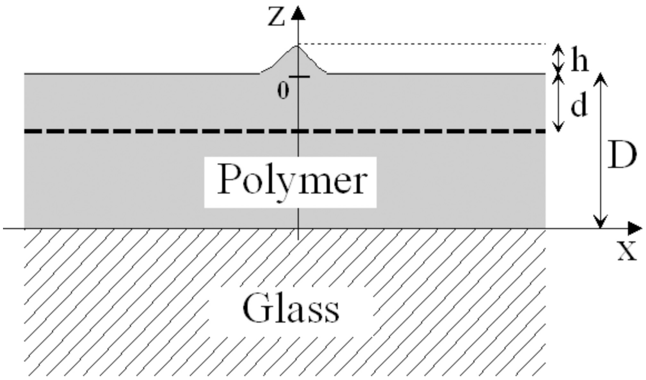

**Fig. 6.** Representation of the quantities involved into the mass migration phenomenon: the dot height (*h*); the thickness of the material that participates to the surface relief formation (*d*); the thickness of the polymer film (*D*).

condition, we have found no embossing of the sample surface, confirming that the writing phenomenon is only due to light absorption by the azo-molecules.

The inset of Fig. 4 shows the first two seconds of the dot formation. We are sensitive to the dot formation from the early state of the mass migration phenomenon because the data sampling and the feedback time constant are of the order of few milliseconds. Furthermore, with the set-up described here, we tested to be able to appreciate surface protrusions lower than 3 nm during scanning of the sample surface.

After stabilizing the sample temperature, we have drawn several dots in areas of $6 \times 6\ \mu\mathrm{m}^2$ or $8 \times 8\ \mu\mathrm{m}^2$ and in several regions of the sample surface in order to feed the statistic with an ensemble of dots representative of the sample. Finally, we have changed the sample temperature, in order to analyze the temperature effects on the dynamic of the dot growth.

Figure 5 reports the dot height versus the exposure time for a 50/50 PMA/PMA4 copolymer film in correspondence of sample temperatures of 30°C, 45°C and 60°C. The value of the glass transition temperature of 50/50 copolymer should be around 50°C. The dot height decreases as the sample temperature increases. This behaviour is expected owing to the decreasing of the sample viscosity corresponding to the temperature increasing. This aspect has been further analyzed by means of the fitting procedure proposed later.

## Analysis and results

To describe the temporal trend of the dot growth and use an expression to fit the data, we referred to a model developed by Barret *et al.* that is based on the idea that the mass migration that leads to the formation of dots can be modelled as the motion of a Newtonian fluid in the classical laminar flow regime (Barrett *et al.*, 1998; Sumaru *et al.*, 2002). This model starts from the Navier–Stokes equations for the description of the material motion, considering a two-dimensional system composed of the vertical dimension ($z$) and one horizontal dimension ($x$), assuming that a similar process occurs in the other coordinate (Fig. 6). The final growing trend derived by Barrett *et al.* (1998) predicts a rate of variation of the film thickness ($h_\mathrm{F}$) of the form $\partial h_\mathrm{F}/\partial t \propto h^3{}_\mathrm{F}$. Starting from this expression, we found that best fit to our data is obtained by using the expression

$$h(t) = d - \frac{d}{\sqrt{1 + \frac{2}{3}\beta d^2 t}}, \qquad (1)$$

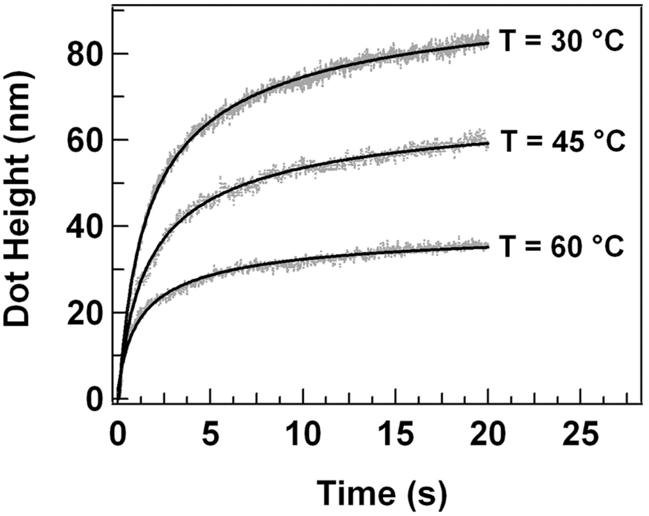

**Fig. 7.** Plots of the experimental data (grey) and the derived fitting functions (black solid lines) described by Eq. (1).

**Table 1.** Mean values of the fitting parameters *d* and $\tau$ obtained in correspondence of different sample temperature regimes.

| Temperature (°C) | *d* (nm) | $\tau$ (s) |
|---|---|---|
| 30 | 86 ± 9 | 11 ± 2 |
| 45 | 64 ± 7 | 11.8 ± 1.6 |
| 60 | 47 ± 7 | 12 ± 2 |

where $h$ is the dot height measured from the sample surface ($z = 0$, Fig. 6), $\beta$ is a constant that can be considered dependent on the value of the sample viscosity and the spatial derivative of the force that drives the mass displacement (Barrett *et al.*, 1998), $d$ is the asymptotic height of the grown dot, $t$ is the exposure time. In Fig. 6, the sample thickness is labelled with letter $D$, whereas $d$ indicates the thickness of the portion of the sample involved in the mass migration. In principle, not all of the material participates in the mass migration and it is impossible to know *a priori* the value of $d$. This reasoning is also in accordance with the localized nature of the near-field radiation and the strong absorption exhibited by azo-based polymers that may limit the portion of material involved.

Results of the fitting procedure, where we left $\beta$ and $d$ as fitting parameters, are displayed in Fig. 7. The black solid lines represent the functions derived by fitting our data with Eq. (1). The accordance between theoretical description and experimental data is excellent for all the explored temperature regimes.

To make possible a direct comparison of the fitting parameters with the experimental data, in Table 1 we report the values for $d$ and $\tau$ (instead of $d$ and $\beta$) as results from fitting. Here $\tau$ represents the time necessary for $h(t)$ to reach the 90% of its final value after light exposure for 20 s ($h(t = \tau) = 90\%$ $h(t = 20$ s)). Thus, $\tau$ can be regarded as the time constant of the process and results in a combination of the original fitting parameters $d$ and $\beta$.

The values reported in Table 1 for $d$ and $\tau$ are obtained averaging over all the values obtained for all the dots drawn at a fixed temperature. We have noted a decreasing of the asymptotic value of the dot height ($d$) as the sample temperature increases. This behaviour is expected owing to the decreasing of the sample viscosity as the temperature increases. Although Eq. (1) fits the experimental data well, it only describes the early state of the SRF phenomenon. This is expected owing to the fact that trends like Eq. (1) are derived neglecting restoring forces induced into the material that stop the process before reaching the maximum available displacement (Barrett *et al.*, 1998; Sumaru *et al.*, 2002); thus, it well applies only to the early state of the phenomenon. Models accounting for the complete evolution of the growth are a hard topic, not unravelled yet. Considering more forces greatly complicates the mathematical formalism and the data interpretation because these forces have different natures and depend on the material characteristics. Nevertheless, we have checked that in our experimental conditions, the early state is represented by the first 20 s in the dot growth (coinciding to the exposure time we have used). Light exposure for longer time leads to the appearance of a different trend in the growing process after 20 s. Expression (1) would better describe an ideal process that takes place until all the material in the thickness $d$ has been displaced.

However, data derived by our procedure are useful indeed because there is much interest in studying the early state of the mass migration that is less influenced by material-specific properties and experimental conditions. Hence, our investigation provides, for the first time, a complete analysis of the mass migration phenomenon from its early state.

## Conclusion

The dynamic of dot growth in azo-containing polymers after illumination with laser light through a SNOM probe is investigated. The excellent agreement found in our analysis between experimental data and a fitting procedure based on a model developed in Barrett *et al.* (1998) is a proof of the accuracy we have achieved in the measurement. SNOM is suitable to investigate the dynamic of the mass migration owing to the local illumination that it provides together with the constant monitoring of the tip-to-sample distance via the feedback circuit. The topic of the origin of the surface relief formation is still a matter of discussion and far from a complete understanding. In this scenario, our investigation also constitutes the first experimental investigation of the dot growth during the early state of the light–polymer interaction. Thus, our results can be considered as an important reference for any future experimental investigation or theoretical description of the surface relief formation on azo-based polymers.

## Acknowledgements

We are grateful to G. Galli for the PMA/PMA4 synthesis, to A. Arena for the preparation of the spin-coated samples and to F. Fuso and O. Esenturk for helpful discussions and advices. We also thank Nanotec Electronica for providing us the software for image processing.

## References

Ambrosio, A., Allegrini, M., Latini, G. & Cacialli, F. (2005) Thermal processes in metal-coated fiber probes for near-field experiments. *Appl. Phys. Lett.* **87**, 033109.

Andreozzi, L., Camorani, P., Faetti, M. & Palazzuoli, D. (2002) Optical bit stability and relaxation processes in a liquid crystal polymer with a photosensitive azo dye molecule as side group. *Mol. Cryst. Liq. Cryst.* **375**, 129–142.

Barrett, C.J., Natansohn, A.L. & Rochon, P.L. (1996) Mechanism of optically inscribed high-efficiency diffraction gratings in azo polymer films. *J. Phys. Chem.* **100**, 8836–8842.

Barrett, C.J., Rochon, P.L. & Natansohn, A.L. (1998) Model of laser-driven mass transport in thin films of dye-functionalized polymers. *J. Chem. Phys.* **109**, 1505–1516.

Bian, S., Williams, J.M., Kim, D.Y., Li, L., Balasubramanian, S., Kumar, J. & Triphathy, S. (1999) Photoinduced surface deformations on azobenzene polymer films. *J. Appl. Phys.* **86**, 4498–4508.

Davy, S. & Spajer, M. (1996) Near field optics: snapshot of the field emitted by a nanosource using a photosensitive polymer. *Appl. Phys. Lett.* **69**, 3306–3308.

Gucciardi, P.G., Patanè, S., Ambrosio, A., *et al.* (2005) Observation of tip-to-sample heat transfer in near-field optical microscopy using metal-coated fiber probes. *Appl. Phys. Lett.* **86**, 203109.

Hasegawa, M., Ikawa, T., Tsuchimori, M., Watanabe, O. & Kawata, Y. (2001) Topographical nanostructure patterning on the surface of a thin film of polyurethane containing azobenzene moiety using the optical near field around polystyrene spheres. *Macromolecules* **34**, 7471–7476.

Holme, N.C.R., Nikolova, L., Hvilsted, S., Rasmussen, P.H., Berg, R.H. & Ramanujam, P.S. (1999) Optically induced surface relief phenomena in azobenzene polymers. *Appl. Phys. Lett.* **74**, 519–521.

Jiang, X.L., Li, L., Kumar, J., Kim, D.Y., Shivshankar, V. & Tripathy, S.K. (1996) Polarization dependent recordings of surface relief gratings on azobenzene containing polymer films. *Appl. Phys. Lett.* **68**, 2618–2620.

Kim, D.Y., Li, L., Jiang, X.L., Shivshankar, V., Kumar, J. & Tripathy, S.K. (1995a) Polarized laser induced holographic surface relief gratings on polymer films. *Macromolecules* **28**, 8835–8839.

Kim, D.Y., Tripathy, S.K., Li, L. & Kumar, J. (1995b) Laser-induced holographic surface relief gratings on nonlinear optical polymer films. *Appl. Phys. Lett.* **66**, 1166–1168.

Kumar, G.S. & Neckers, D.C. (1998) Photochemistry of azobenzene-containing polymers. *Chem. Rev.* **89**, 1915–1925.

Labardi, M., Coppedè, N., Pardi, L., *et al.* (2003) Sub-micron scale optical read/write/erase on azo-polymethacrylate thin films by scanning near-field optical microscopy. *Mol. Cryst. Liq. Cryst.* **398**, 33–43.

Landraud, N., Peretti, J., Chaput, F., Lampel, G., Boilot, J.-P., Lahlil, K. & Safarov, V.I. (2001) Near-field optical patterning on azo-hybrid sol–gel films. *Appl. Phys. Lett.* **79**, 4562–4564.

Latini, G., Downes, A., Fenwick, O., *et al.* (2005) Optical probing of sample heating in scanning near-field experiments with apertured probes. *Appl. Phys. Lett.* **86**, 011102.

Likodimos, V., Labardi, M., Pardi, L., Allegrini, M., Giordano, M., Arena, A. & Patanè, S. (2003) Optical nanowriting on azobenzene side-chain polymethacrylate thin films by near-field scanning optical microscopy. *Appl. Phys. Lett.* **82**, 3313–3315.

Patanè, S., Arena, A., Allegrini, M., Andreozzi, L., Faetti, M. & Giordano, M. (2002) Near-field optical writing on azo-polymethacrylate spin-coated films. *Opt. Commun.* **210**, 37–41.

Sumaru, K., Fukuda, T., Kimura, T., Matsuda, H. & Yamanaka, T. (2002) Photoinduced surface relief formation on azopolymer films: a driving force and formed relief profile. *J. Appl. Phys.* **91**, 3421–3430.

Viswanathan, N.K., Balasubramanian, S., Li, L., Kumar, J. & Tripathy, S.K. (1998) Surface-initiated mechanism for the formation of relief gratings on azo-polymer films. *J. Phys. Chem. B* **102**, 6064–6070.